

Ion-induced triple fragmentation of CO_2^{3+} into $\text{C}^+ + \text{O}^+ + \text{O}^+$ M. R. Jana,^{1,*} P. N. Ghosh,² B. Bapat,³ R. K. Kushawaha,³ K. Saha,³ I. A. Prajapati,³ and C. P. Safvan⁴¹*Department of Physics, University of Calcutta, 92, A. P. C. Road, Kolkata 700009, India*²*Jadavpur University, 188, Raja S C Mallick Road, Kolkata 700032, India*³*Physical Research Laboratory, Ahmedabad 380009, India*⁴*Inter-University Accelerator Centre, Aruna Asaf Ali Marg, New Delhi 110067, India*

(Received 1 September 2011; published 27 December 2011)

Dissociation of CO_2^{3+} formed in fast, heavy-ion-induced ionization of CO_2 , using $5 \text{ MeV u}^{-1} \text{ Si}^{12+}$ ions as projectiles, has been studied by the technique of multi-ion coincidence momentum imaging. From the momentum correlation between the ejected ions, we conclude that dissociation of CO_2^{3+} into $\text{C}^+ + \text{O}^+ + \text{O}^+$ is a concerted process involving linear and bent conformations of CO_2^{3+} . The kinetic-energy-release spectrum of the dissociation channel $\text{CO}_2^{3+} \rightarrow \text{C}^+ + \text{O}^+ + \text{O}^+$ is measured and the possible excited states of CO_2^{3+} are computed *ab initio*.

DOI: [10.1103/PhysRevA.84.062715](https://doi.org/10.1103/PhysRevA.84.062715)

PACS number(s): 34.50.-s, 82.80.Rt, 33.15.-e

I. INTRODUCTION

Highly charged ions colliding with molecules are capable of producing highly charged transient molecular ions, mainly via valence-charge stripping [1,2]. In the case of swift projectiles, electron removal from a fixed-in-space molecule results in transitions to the excited states of the transient molecular ion at the equilibrium internuclear distance (R_e) of the neutral molecule. The relaxation of the deposited energy then leads to molecular fragmentation. When the interaction time is much smaller than the typical vibrational and rotational time periods of a molecule, the excitation is a Franck Condon process and the kinetic energy release (KER) of the fragments directly reflects the properties of the dissociative state of the multiply ionized molecule. For highly charged fragments, the mean KER values can be well reproduced by calculating the potential energy of pointlike charges separated by R_e . This simple two-step fragmentation model is not applicable at low impact velocities, where postcollision interaction effects involving the projectile play an important role in the overall collision dynamics. Understanding molecular fragmentation dynamics by obtaining detailed potential energy surfaces of the transient species is one of the current pursuits of chemists and physicists [3,4].

In collisions with fast projectiles, direct ionization is the dominant process of electron removal, in contrast with the case of low-energy projectiles where electron capture and transfer ionization are the dominant processes [5–7]. Many-body fragmentation proceeds via regions of densely populated potential energy surfaces which support many transitions [8]. Ion-induced molecular fragmentation studies in different energy regimes have shown that electron removal due to capture results in weaker excitation of the target than direct ionization [9] and these energy regimes give information about the different excited electronic states of a given multiply charged molecular ion.

Fragmentation of CO_2 is a much-studied topic, with synchrotron radiation [10,11], electron impact [12], fast heavy-ion beams [13], slow highly charged ions [8], as well as with intense lasers [14–16] having been employed as

perturbations. Many theoretical studies for the electronic states of neutral [17,18], singly [19], and doubly charged [20,21] CO_2 molecular ions have been reported in the literature, but the potential energy surfaces of CO_2^{3+} are largely unexplored.

We report here a study of triple fragmentation of CO_2 into three ionic fragments via the channel $\text{CO}_2^{3+} \rightarrow \text{C}^+ + \text{O}^+ + \text{O}^+$. In the experiment, a beam of neutral CO_2 molecules crossed a beam of $5 \text{ MeV u}^{-1} \text{ }^{28}\text{Si}^{12+}$ ions and the fragments were analyzed by an ion momentum spectrometer. Supporting the analysis of the experimental kinetic energy data were *ab initio* quantum chemical computations to obtain the potential energy levels of CO_2^{3+} ions. The projectile speed translates to an interaction time of 17 attoseconds, which is much shorter not only than the typical rotational and vibrational time periods of the molecule, but also than the typical fragmentation times of the molecules (around 10 fs). We thus have access to the molecular ion in its vibrationally frozen state devoid of any interference from the projectile electric field. The molecular core can be assumed to be frozen during the interaction, and the kinetic energy distribution of the fragments can be expected to reflect the properties of the states of the multiply ionized molecule.

We compare the results of our work (using $5 \text{ MeV u}^{-1} \text{ Si}^{12+}$) with those of Adoui *et al.* ($8 \text{ MeV u}^{-1} \text{ Ni}^{24+}$) [3], Siegmann *et al.* ($5.9 \text{ MeV u}^{-1} \text{ Xe}^{18+}$ and Xe^{43+}) [13], and Neumann *et al.* ($3.2 \text{ keV u}^{-1} \text{ Ar}^{8+}$) [8], which involve collisions with widely differing interaction times and perturbation strengths. These cases correspond, in terms of the interaction times, to 17 as, 13 as, 16 as, and 680 as, respectively, and in terms of the perturbation strength q/v to 0.85, 1.34, 1.17, 2.80, and 22.3, respectively.

II. EXPERIMENT AND DATA ANALYSIS

Details of the experimental apparatus and data acquisition methodology for molecular fragmentation studies used in this experiment have been described elsewhere [22]. The experiment was performed using ion beams from the Pelletron accelerator at the Inter University Accelerator Centre [23]. Here we give a brief description of the setup. Projectile ions were transported to the collision chamber where they interacted with a beam of neutral molecules effusing from a

*ecstasy.mridula@gmail.com

capillary in a crossed-beam geometry. An ion current of a few pA was maintained during the experiments. The low current is necessary to keep the accidental coincidences at an acceptable rate. The vacuum in the main chamber was 7×10^{-8} mbar without the target molecular beam and around 5×10^{-7} mbar with the target molecular beam. The target gas number density was approximately 10^{12} – 10^{13} cm^{-3} . The stagnation pressure behind the capillary was approximately 1.4 mbar, and the delivery lines were maintained at room temperature.

The coincidence momentum imaging technique is based on the principle of simultaneous measurement of ion time of flight (TOF) and spatial spread transverse to the flight direction under the action of a uniform electric field. For guiding the ions and electrons generated in the collision zone, a uniform electric field is generated by a set of parallel rings in a potential divider arrangement. The rings at the ends have wire meshes on them to ensure field uniformity. The field of strength 140 V cm^{-1} is applied over a length of 99 mm in a direction perpendicular to the plane formed by the crossed ion beam and gas jet. Ions travel through this field, followed by a field-free drift region of length 198 mm before hitting the detector. At the exit of the drift tube, the ionic fragments are detected by a microchannel plate detector (MCP). Ejected electrons are extracted in the direction opposite to that of the ions and detected using another MCP. The pulse from the latter MCP acts as the start trigger for the multihit ion TOF measurement. TOF of ions is determined by an electron-ion coincidence and recorded by a multistop time-to-digital converter. The timing and position data are written event by event into a list mode file. The event rate during the data acquisition was approximately 500–600 Hz.

The recorded data are analyzed offline. The observed flight time t and the position (x, y) information for each ion in an event is transformed to yield the three-momentum components for each ion. The multihit capability of the acquisition system permits detection and determination of the momentum of up to four ions from the same event. From this multihit data, further information about the fragmentation process such as the angle of ejection, kinetic energy of fragments, etc. is derived.

III. RESULTS AND DISCUSSIONS

A. Fragmentation Channels

CO_2^{3+} may fragment via various channels, with several fragment combinations being possible. From the analyzed data we discern the following four fragment triplets (the neutral being undetected, but deduced by analysis): (i) $\text{C}^{2+} : \text{O}^+ : \text{O}$, (ii) $\text{C} : \text{O}^{2+} : \text{O}^+$, (iii) $\text{C}^+ : \text{O}^{2+} : \text{O}$, and (iv) $\text{C}^+ : \text{O}^+ : \text{O}^+$.

From the triple-ion coincidence map (Fig. 1), we find O^+ to be the third ion, implying a $\text{C}^+ : \text{O}^+ : \text{O}^+$ breakup. While the $\text{C}^+ : \text{O}^+$ coincidence may arise from the breakup of molecular ions other than CO_2^{3+} , we can separate out the contribution of CO_2^{3+} in the $\text{C}^+ : \text{O}^+$ coincidence by applying suitable conditions on the event list. This channel is the dominant triple fragmentation channel of CO_2^{3+} in the present case and is the focus of our attention.

Dissociation of a triatomic molecule into three atomic or ionic fragments may take place either by simultaneous breaking of the bonds (the two C–O bonds in case of CO_2), called a concerted breakup, or by a sequential breakup of the two bonds. In a sequential breakup the time interval between two successive bond breaks is of the order of the rotational time period.

B. Triple-fragmentation kinematics

Figure 2 (left) shows momentum correlation between the three fragments of CO_2^{3+} , where the arrow represents direction of the momentum of the first fragment (C^+) and is taken as the reference direction. The components of momentum of the second and third fragments (O^+ in both cases) parallel and perpendicular to it are obtained, and the events are histogrammed as two-dimensional (2D) momentum plot. The distributions of both O^+ ions are single lobed and nearly identical. The similarity is further seen in the individual kinetic energy spectra of the two O^+ ions [Fig. 2 (right)]. The O^+ kinetic energy distributions are broad and peak around 15 eV. In contrast, the corresponding C^+ kinetic energy distribution is narrow and peaks at slightly over 1 eV. Our result is in very

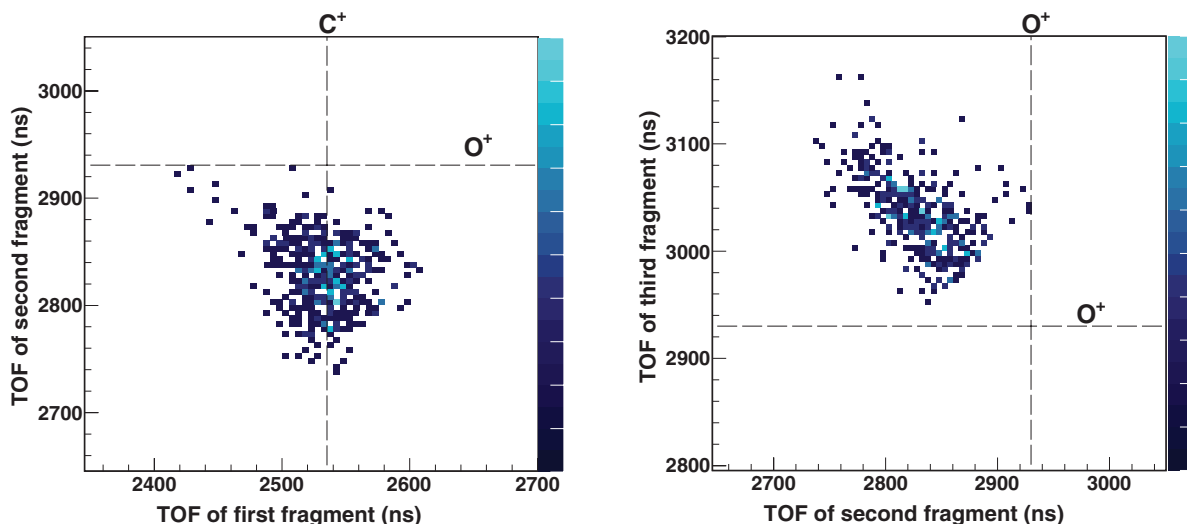


FIG. 1. (Color online) Coincidence map of (left) first and second fragments and (right) second and third fragments corresponding to $\text{CO}_2^{3+} \rightarrow \text{C}^+ : \text{O}^+ : \text{O}^+$ channel. The dashed lines drawn correspond to the peak of the respective ions in the TOF spectrum.

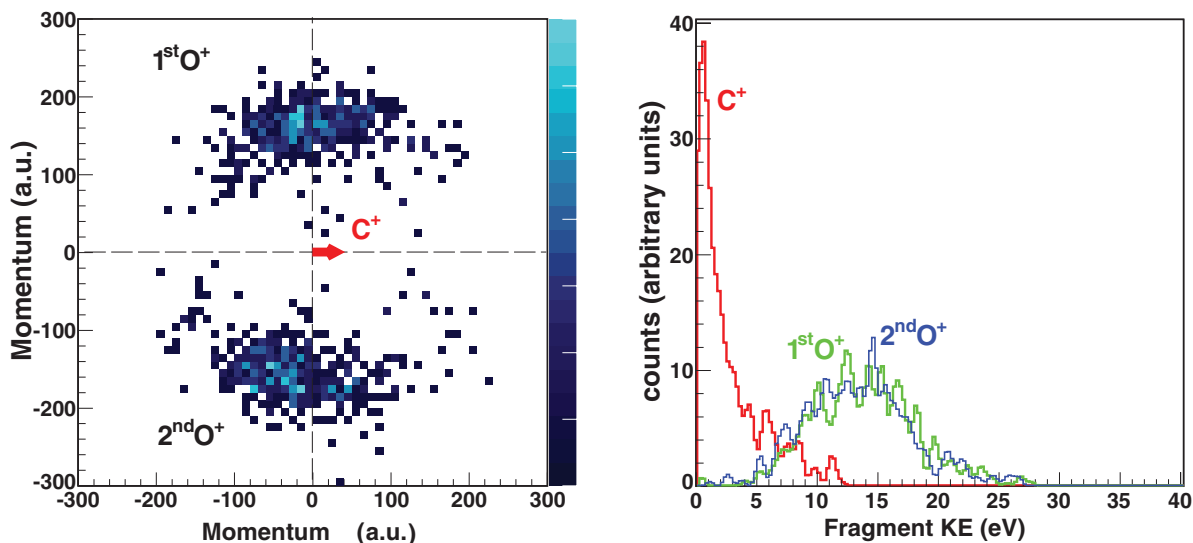


FIG. 2. (Color online) (left) Correlated momentum map of C^+ , O^+ , and O^+ ions from dissociation of CO_2^{3+} . (right) Kinetic energies of individual ions for the same channel.

good agreement with that obtained by Siegmann *et al.* where $5.9 \text{ MeV u}^{-1} \text{ Xe}^{43+}$ were used as projectiles [see Fig. 7 (top) in [13]].

If the two oxygen ions separate out symmetrically, the central carbon ion will have zero momentum in case the separation takes place from a linear geometry. The observed nonzero kinetic energy of C^+ is a consequence of the $\text{O}-\text{C}-\text{O}$ bond angle in the fragmentation complex being $<180^\circ$. The most probable $\text{O}-\text{C}-\text{O}$ bond angle in an ensemble of CO_2 molecules, taking into account zero-point vibrational excitations, is 172.5° [13]. The asymptotic angle between the momentum vectors of the two O^+ ions originating from such a state will, in the case of concerted dissociation, be smaller than the initial $\text{O}-\text{C}-\text{O}$ bond angle due to the Coulomb repulsion between the three fragments, resulting in a distribution with

the modal value being $<172.5^\circ$. This is clearly seen in the triple-ionization results of Kushawaha *et al.*, Adoui *et al.*, and Siegmann *et al.* (in particular, see Fig. 8 in [3] and Fig. 4 in [10]). There may be other reasons for broadening, such as dissociation from a bent electronic state. In the present case the distribution of the angle between the two O^+ momentum vectors peaks at about 165° [Fig. 3 (left)] with a long tail extending to angles as small as 60° , and a minor peak around 135° . The magnitude of the momenta carried away by the two O^+ ions are nearly identical. The combined implications of the observations regarding the relative emission angles and the kinetic energy distributions is that we have here a concerted fragmentation, from linear as well as bent states of CO_2^{3+} .

Results from Siegmann *et al.* ($5.9 \text{ MeV u}^{-1} \text{ Xe}^{18+}$ and Xe^{43+} impact) show that, in case of $\text{O}^+\text{C}^+\text{O}^+$ fragmentation,

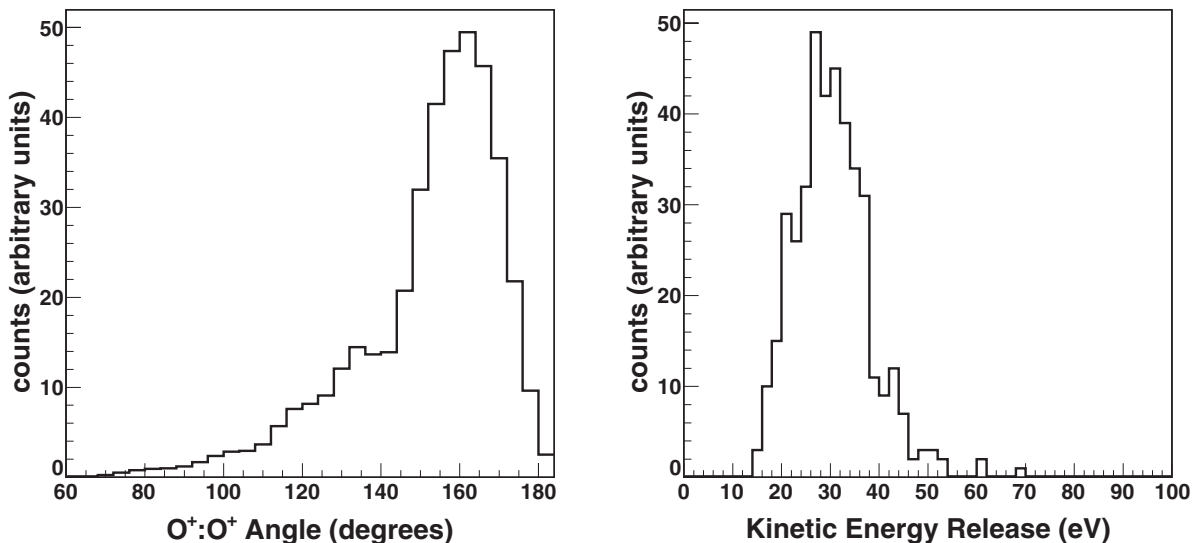


FIG. 3. (left) Distribution of the angle between the momentum vectors of the two O^+ ions. (right) KER of CO_2^{3+} dissociating into $\text{O}^+ + \text{C}^+ + \text{O}^+$. The KER distribution is similar in swift-collision cases [3,13] is narrower for slow projectiles [8].

the distribution of the $O^+ : O^+$ angle peaks at 120° [see Figs. 5 (right) and 6 (top left) in [13]] for both charge states, and those distributions are broader than in the present case. On the other hand, the results of Adoui *et al.* show a peak around 165° , tailing off at about 120° (see Fig. 8 in [3]), and the distribution is narrower than the present case. This comparison shows that both projectile charge state and projectile speed influence the distribution of the $O^+ : O^+$ angle. The distribution of this angle in all cases deviates from that expected in a pure Coulomb explosion model, which means that excited-state potential energy surfaces play a significant role in determining the angular distributions. The observed influence of the projectile charge and speed on the angular distributions is consistent with the fact, that different projectile charge states and speeds will lead to different distributions of excited states.

The KER distribution [Fig. 3 (right)] of $CO_2^{3+} \rightarrow C^+ + O^+ + O^+$ channel shows signature of three peaks at 20.7 eV, 26.8 eV, and 30.8 eV with some minor higher-energy peaks in the region 15–55 eV. These peaks can have their origin in the shallow electronic states of the parent molecular ion. We have analyzed the KER distribution as a function of $O^+ : O^+$ angle in the two ranges 60° – 140° and 140° – 180° and found that the KER distributions in the two cases are not significantly different. The KER distributions in the other swift-ion-collision cases (Siegmann *et al.*, Adoui *et al.*) and the present case are quite similar. Within the range of projectile charge states for swift ions compared here, there is no significant dependence of the KER distributions on the projectile charge state. The case of slow collisions (Neumann *et al.*) is different, with the KER spectrum showing a broad peak around 20.6 eV with a high-energy tail extended up to 40 eV. The data of Neumann *et al.*, shows a mixture of processes. In that case the interaction time was much longer than present, allowing for vibrational and rotational relaxation during the collision. In particular, when analyzed as a function of the KER, their data show the following: For $KER = 17 \pm 0.5$ eV, the breakup is predominantly sequential type where ejection of one O^+ from CO_2^{3+} leaves behind a rotating CO_2^{2+} ion which fragments after a time delay. The circular momentum distribution in the Newton diagram (Fig. 2 in [8]) is a proof of this sequential mechanism. On the other hand, concerted breakup is the dominant mechanism for $KER = 31 \pm 0.5$ eV and $KER = 38 \pm 0.5$ eV. Within the range of perturbations compared here, the KER distribution is the same for all swift collisions ($14 \text{ a.u.} < v < 18 \text{ a.u.}$), irrespective of the projectile charge ($12 < q < 43$). In slow collisions, excited states that lead to sequential dissociation are accessed, leading to a different KER distribution as compared with swift collisions.

C. Computed KER values

A simple Coulomb explosion model of the triple-ion breakup, assuming an initial separation of 120 pm between the C and O nuclei in the CO_2^{3+} molecular ion in a linear state yields a KER of 30 eV [11]. Under the same approximation, but from a bent state, the KER would be higher. The range of KER values arises from various possibilities: bent initial states, crossing of CO_2 and CO_2^{3+} potential energy surfaces, etc. These are investigated by *ab initio* computations of the

TABLE I. Possible molecular states of linear CO_2^{3+} dissociating into $C^+ + O^+ + O^+$ along with the theoretically calculated values of KER.

| Molecular states | Release energy (eV) | Dissociation limit |
|------------------|---------------------|----------------------------------|
| $^2\Pi$ | 20.6 | $C^+(^4P) + O^+(^2D) + O^+(^2D)$ |
| | 24.4 | $C^+(^2P) + O^+(^2D) + O^+(^2D)$ |
| | 25.8 | $C^+(^4P) + O^+(^4S) + O^+(^2D)$ |
| | 29.3 | $C^+(^2P) + O^+(^4S) + O^+(^2D)$ |
| | 34.5 | $C^+(^2P) + O^+(^4S) + O^+(^4S)$ |
| $^4\Sigma$ | 15.9 | $C^+(^4P) + O^+(^2D) + O^+(^2D)$ |
| | 19.7 | $C^+(^2P) + O^+(^2D) + O^+(^2D)$ |
| | 24.6 | $C^+(^2P) + O^+(^2D) + O^+(^4S)$ |
| | 26.3 | $C^+(^4P) + O^+(^4S) + O^+(^4S)$ |

potential energy curves for the low-lying states of the CO_2^{3+} molecular ion. The unrestricted Hartree-Fock (UHF) energies are calculated at the internuclear distance of CO_2^{3+} with a 6-311G basis set including diffused $sp(L)$ shell using the GAMESS package [24]. With our preliminary calculations we found the existence of shallow (possibly metastable) electronic states of CO_2^{3+} molecular ion whose dissociation can lead to sharp peaks in the KER spectra. The appearance of peaks in the KER distribution, whose origin lies in these shallow electronic states, depends on the population of other excited states of the parent molecular ion.

Table I lists possible molecular states of CO_2^{3+} dissociating into various states of C^+ , O^+ , and O^+ along with the KER values obtained by UHF calculations. In these calculations CO_2^{3+} is taken to have a linear geometry. The calculated KER values span the energy range observed in the experiment, and the dominant fragmentation channels may be tagged to the observed KER from Table I.

The high-energy components (36.7, 42.7, 50.0 eV, etc.) cannot be explained from the low lying $^4\Sigma$ and $^2\Pi$ states of CO_2^{3+} . These may arise from the higher excited states of the precursor molecular ion.

A close inspection of the KER distribution for the $C^+ : O^+ : O^+$ channel seen in 3.2 keV u^{-1} Ar^{8+} impact on CO_2 shows a broad peak around 20.6 eV and other less prominent peaks at 19, 22, and 24 eV. These peaks lie well within the range of our computed values considering linear structure of the CO_2^{3+} ion.

IV. CONCLUSION

In this article, we have analyzed different dissociation pathways of triply charged CO_2 molecular ions, formed in collisions between neutral CO_2 molecules and 5 MeV u^{-1} Si^{12+} ions, into $C^+ : O^+ : O^+$ channel. The KER spectrum of this particular channel has multiple peaks. The range of measured KER values is well explained from our *ab initio* quantum chemical calculations, although more detailed calculations are clearly called for to reproduce the entire KER distribution. The range of angles between the momentum vectors of the two O^+ ions is greater than that governed by vibrational modes of the linear state, implying participation

of the bent electronic states in dissociation of CO₂³⁺. The contribution from bent electronic states is evident from the small peak around 135° and a pronounced tail below 140° in the O⁺ : O⁺ angular distribution [Fig. 3 (left)]. Comparison of the breakup pattern of CO₂³⁺ induced by various perturbations shows differences: the swift perturbations almost exclusively lead to concerted triple-ion breakup, but significant probability for stepwise breakup is seen with slow perturbations.

ACKNOWLEDGMENTS

We thankfully acknowledge the staff of Inter-University Accelerator Centre and Pelletron group for providing all necessary facilities. M.R.J. thanks the UGC for providing financial support. C.P.S acknowledges the support of Department of Science and Technology, Government of India for funding the High Performance Computing Centre (Grant No. IR/S2/PF-02/2007).

-
- [1] L. Adoui *et al.*, *Phys. Scr. T* **92**, 89 (2001).
[2] J. H. Sanderson, T. Nishide, H. Shiromaru, Y. Achiba, and N. Kobayashi, *Phys. Rev. A* **59**, 4817 (1999).
[3] L. Adoui *et al.*, *Nucl. Instrum. Methods Phys. Res., Sect. B* **245**, 94 (2006).
[4] C. P. Safvan and D. Mathur, *J. Phys. B* **27**, 4073 (1994).
[5] P. Sobocinski, Z. D. Pešić, R. Hellhammer, D. Klein, B. Sulik, J.-Y. Chesnel, and N. Stolterfoht, *J. Phys. B* **39**, 927 (2006).
[6] G. Sampoll, R. L. Watson, O. Heber, V. Horvat, K. Wohrer, and M. Chabot, *Phys. Rev. A* **45**, 2903 (1992).
[7] J. Rajput, S. De, A. Roy, and C. P. Safvan, *Phys. Rev. A* **74**, 032701 (2006).
[8] N. Neumann *et al.*, *Phys. Rev. Lett.* **104**, 103201 (2010).
[9] M. Tarisien *et al.*, *J. Phys. B* **33**, L11 (2000).
[10] R. K. Kushawaha, S. Sunil Kumar, I. A. Prajapati, K. P. Subramanian, and B. Bapat, *J. Phys. B* **42**, 105201 (2009).
[11] R. K. Singh, G. S. Lodha, V. Sharma, I. A. Prajapati, K. P. Subramanian, and B. Bapat, *Phys. Rev. A* **74**, 022708 (2006).
[12] C. Tian and C. R. Vidal, *Phys. Rev. A* **58**, 3783 (1998).
[13] B. Siegmann, U. Werner, H. O. Lutz, and R. Mann, *J. Phys. B* **35**, 3755 (2002).
[14] C. Cornaggia, M. Schmidt, and D. Normand, *J. Phys. B* **27**, L123 (1994).
[15] A. Hishikawa, A. Iwamae, and K. Yamanouchi, *Phys. Rev. Lett.* **83**, 1127 (1999).
[16] G. Ravindra Kumar, P. Gross, C. P. Safvan, F. A. Rajgara, and D. Mathur, *Phys. Rev. A* **53**, 3098 (1996).
[17] Sotiris S. Xantheas, S. T. Elbert, and Klaus Ruedenberg, *Chem. Phys. Lett.* **166**, 39 (1990).
[18] Nicholas Wilhelm Winter, Charles F. Bender, and William A. Goddard III, *Chem. Phys. Lett.* **20**, 489 (1973).
[19] K. E. McCulloh, *J. Chem. Phys.* **59**, 4250 (1973).
[20] M. Hochlaf, F. R. Bennett, G. Chambaud, and P. Rosmus, *J. Phys. B* **31**, 2163 (1998).
[21] H. Hogueve, *J. Phys. B* **28**, L263 (1995).
[22] R. K. Kushawaha, S. Sunil Kumar, M. R. Jana, I. A. Prajapati, C. P. Safvan, and B. Bapat, *J. Phys. B* **43**, 205204 (2010).
[23] D. Kanjilal, S. Chopra, M. M. Narayanan, I. S. Iyer, V. Jha, R. Joshi, and S. K. Datta, *Nucl. Instrum. Methods Phys. Res., Sect. A* **328**, 97 (1993).
[24] M. W. Schmidt, *J. Comput. Chem.* **14**, 1347 (1993).